$[Co/Fe(\alpha\text{-alkyl-tpdt})_2]^{x-}$: Alkyl Substituted Cobalt and Iron Bis-Dithiolenethiophenic Complexes.

Rafaela A. L. Silva,[†] Rodrigo Santos,[†] Marta M. Andrade,[†] Isabel C. Santos,[⊥,†] Joana T. Coutinho,[†] Laura C. J. Pereira,[⊥,†] João C. Waerenborgh,[⊥,†] Bruno J. C. Vieira,[†] Jordi Cirera,[§] Eliseo Ruiz,[§] Manuel Almeida[⊥,†] and Dulce Belo*[,†]*

† C^2TN, Instituto Superior Técnico, Universidade de Lisboa, Estrada Nacional 10, P-2695-066 Bobadela LRS, Portugal

[⊥] DECN, Departamento de Engenharia e Ciências Nucleares, Instituto Superior Técnico, Universidade de Lisboa, Estrada Nacional 10, P-2695-066 Bobadela LRS, Portugal

§ Departament de Química Inorgànica i Orgànica and Institut de Química Teòrica i Computacional, Diagonal 645, Barcelona, Spain

KEYWORDS. Iron, Cobalt, Dithiolene complexes, Magnetic susceptibility.

ABSTRACT. Tetraphenylphosphonium salts of Co and Fe complexes with alkyl substituted, *tert*-butyl (*tb*) and isopropyl (*dp*), 2,3-thiophenedithiolate (α-tpdt) ligands, namely $TPP[Co(\alpha\text{-}tb\text{-tpdt})_2]$ (**3**), $TPP_2[Fe(\alpha\text{-}tb\text{-tpdt})_2]_2$ (**4a-b**), $TPP[Co(\alpha\text{-}dp\text{-tpdt})_2]$ (**5**) and $TPP[Fe(\alpha\text{-}dp\text{-tpdt})_2]$ (**6**) were prepared and characterized by cyclic voltammetry, single crystal

X-ray diffraction, magnetic susceptibility measurements and ^{57}Fe Mössbauer spectroscopy. Compound **3** and **5** are isostructural with their Au and Ni analogues with a square-planar coordination geometry. Compound **4** presents two polymorphs (**4a**-**b**) both showing a Fe(III) bisdithiolene dimerization. The magnetic susceptibility of **3** and **5** show a behavior dominated by antiferromagnetic interactions, with room temperature magnetic moments of 3.40 μB and 3.36 μB, respectively, indicating that these square-planar Co(III) complexes assume an intermediate spin electronic configuration (S=1) as supported by multiconfigurational DFT calculations.

INTRODUCTION

Transition metal bisdithiolene complexes since their first preparation in 1960s have been the topic of continuous research interest due to a vivid redox behavior together with large structural and magnetic diversity[1] making them relevant for different fields such as conducting or magnetic materials,[1-2] catalysis,[3] bioinorganic chemistry and energy conversion.[4] The interesting properties of these complexes are mainly associated to a non-negligible contribution of the ligands (said to be non-innocent) to the frontier molecular orbitals, therefore making them able to stabilize different oxidation and spin states.[5-9] The role of the ligands and the assignment of the metal oxidation states in these complexes have been since long time topics of considerable debate.[10-13]

While the chemistry of late transition metal bisdithiolene complexes, predominantly with square planar coordination geometry for Ni, Pd, Pt Cu and Au has been intensively developed, the Fe and Co complexes remained significantly less studied. Monoanionic iron bisdithiolene complexes are known to adopt, as an almost universal rule, a dimeric arrangement of distorted square planar units, with iron in a 4+1 coordination geometry. There are only two known exceptions where isolated square planar complexes could be obtained; (n-Bu_4N) [$Fe(qdt)_2$] (qdt= 2,3-quinoxalinedithiolate)

where cation interactions hamper the usual dimerization[14] and [Fe(S_2C_2(p-anisyl)$_2$)$_2$], obtained as a co-crystal due to specific solid state interactions.[15] Monoanionic iron bisdithiolene in solution present a dimerisation equilibrium dependent on the nature of the solvents[16-18] and chemical substituents.[19] Both intermediate spin (S=3/2)[15,20-22] and low spin (S=1/2) configurations[14,16,23] have been ascribed to Fe^{III}(bisdithiolene) monoanionic complexes that in case of dimerisation present antiferromagnetic couplings in the range of ~150-250 K.[18,20,22]

The dimerization of cobalt bisdithiolene complexes is less favored than for iron, and they are known to present a remarkably larger diversity of coordination geometries, ranging from isolated square planar to dimeric,[6,24] trimeric[25] and even polymeric[26] arrangements. The number of cobalt bisdithiolene complexes presenting isolated square planar geometry remains relatively scarce. Although initially speculated that square planar monoanionic Co(III)-bisdithiolene complexes with ligands such as a bdt (1,2-benzenedithiolato) or tdt (3,4-toluenedithiolato) could be either in low spin (S=0)[27] or intermediate spin (S=1) states, it was later clearly shown that the ground state of these monoanionic complexes has a spin triplet S=1 ground state with relatively large zero field splitting D= ~30 cm^{-1}.[28]

Recently we have described several bisdithiolene complexes based on ligands with thiophenic groups and reported Au and Ni monoanionic complexes based on *tert*-butyl and diisopropyl substituted thiophenedithiolate ligands, [M(α-*tb*-tpdt)] and [M(α-*dp*-tpdt)] (α-tpdt=2,3-thiophenedithiolate).[29] Besides an increase of solubility brought by the alkyl substituents their bulky nature play a critical role in the solid state packing pattern and may also influence the coordination geometry restraining by steric hindrances the tendency to dimerization.

In this work we report the corresponding [M(α-*tb*-tpdt)$_2$] and [M(α-*dp*-tpdt)$_2$] complexes with M= Co and Fe, obtained in the monoanionic state. While the iron complexes in spite their poor

stability were found to present the standard dimerization with 4+1 metal coordination geometry, the Co monoanionic complexes are clear examples of cobalt complexes with square planar coordination geometry and an intermediate spin S=1 ground state as predicted by theoretical calculations.

RESULTS AND DISCUSSION

Ketones **1** [30] and **2** [29] were prepared by a previously described Friedel-Crafts alkylation of ketone **I** (Scheme 1).[31] The monoanionic complexes based on alkyl substituted ligands, *tert*-butyl and isopropyl, were isolated as Ph_4P^+ salts following a general common procedure frequently used for the preparation of dithiolene complexes, similar to that already reported Au and Ni analogues under anaerobic conditions.[29,32] These reactions are summarized in Scheme 1. Similarly, to their Au and Ni analogues, the cobalt (**3** and **5**) and iron (**4** and **6**) tetraphenylphosphonium salts are soluble in several organic solvents. While the Co compounds are stable and could be recrystallized from dichloromethane, affording single crystals suitable for X-ray diffraction, the iron complexes were less stable in solution and single crystals suitable for X-ray diffraction could be obtained only for **4** by selection from the direct product of the synthesis. For **6** no crystals suitable for X-ray diffraction could be obtained. The crystals of the iron compounds **4** and **6** are not stable as they change color from shining dark brown to dull black crystals, after storage over a period of a few days.

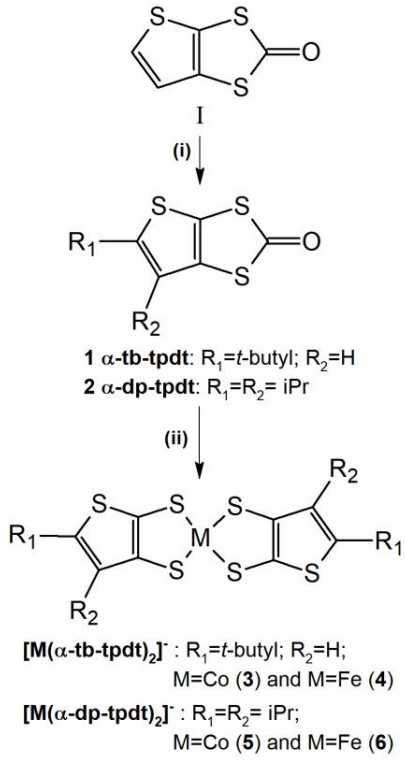

Scheme 1. Synthesis of compounds. i) $AlCl_3$, *tert*-butyl chloride (**1**) or 2-chloropropane (**2**); ii) MeONa/MeOH; $CoCl_2.6H_20$ (**3** and **5**) or $FeCl_3$ (**4** and **6**); TPPBr.

The redox properties of complexes **3**-**6** were studied by cyclic voltammetry in dichloromethane solutions under nitrogen atmosphere. Cobalt compound **5** presents two quasi-reversible processes as shown in Figure 1. Similarly, to closely related bisdithiolene complexes, these waves can be ascribed to the couples dianion/monoanion, at negative potentials, and to monoanion/neutral at positive potentials. In **3**, only a process at negative potentials could be clearly identified, possibly attributed to dianion/monoanion couple with no evidence of oxidation to the neutral species. The corresponding redox potentials are listed in Table 1 in comparison with those of closely related complexes. These results indicate that the Co complex **5** is easier to oxidize to the neutral specie than the non-substituted $[Co(tpdt)_2]^-$ analogue but harder to oxidize than the $[Co(\alpha\text{-}tpdt)_2]^-$. The cyclic voltammograms of Fe complexes **4** and **6,** performed in freshly prepared samples, are in

both cases quite similar with three quasi-reversible processes. The assignment of each process to a redox pair is difficult due to the dimeric nature of these complexes, which are known to be in equilibrium with monomers in solution.[16,33] This assignment is further complicated by the instability of the Fe complex **4** upon air exposure, promptly degrading after one voltammetry sweeping.

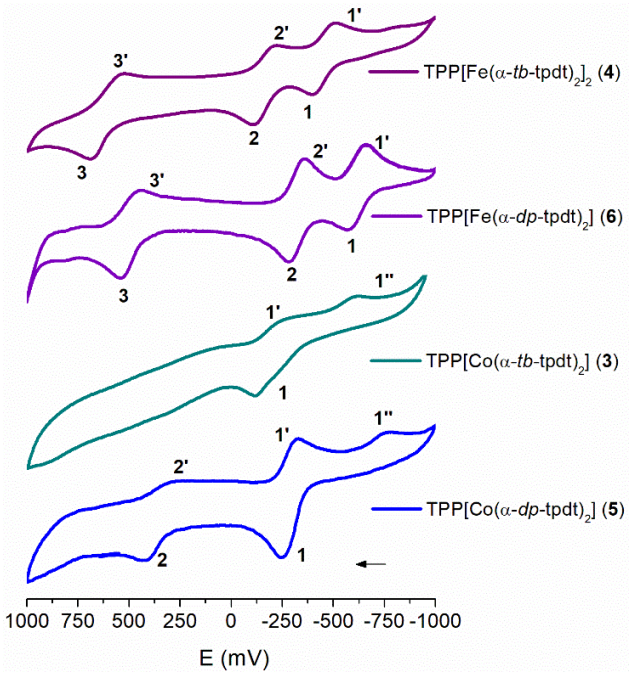

Figure 1. Cyclic voltammetry of **3-6** in dichloromethane solution *vs.* $Ag/AgNO_3$ (scan rate 100 $mV.s^{-1}$).

Table 1. Half wave potentials, $E_{1/2}$ (mV), of cobalt and iron bis-thiophenedithiolene complexes.[a]

Complex	$E^1_{1/2}$ (mV)	$E^2_{1/2}$ (mV)	$E^3_{1/2}$ (mV)	Ref.
$[Co(tpdt)_2]$ [b]	-618	+497	–	34
$[Co(\alpha\text{-tpdt})_2]$ [b]	-591	-257/ -175/ -8	–	34
$[Fe(\alpha\text{-tpdt})_2]$	-65	+232	–	18
$[Co(\alpha\text{-}tb\text{-tpdt})_2]$ (**3**)	-150 (-535)	–	–	This work
$[Co(\alpha\text{-}dp\text{-tpdt})_2]$ (**5**)	-286 (-751)	+367	–	This work
$[Fe(\alpha\text{-}tb\text{-tpdt})_2]$ (**4**)	-458	-165	+612	This work
$[Fe(\alpha\text{-}dp\text{-tpdt})_2]$ (**6**)	-616	-321	+490	This work

[a] $Ag/AgNO_3$ as reference electrode and scan rate 100 $mV.s^{-1}$ with dichloromethane as solvent. Values between brackets are the cathodic peak potential - 1'' in Figure 1 ($E_p^{1''}$). [b] Solvent acetonitrile. Table S1 indicates the Fc/Fc^+ couple that was used as an internal reference.[35]

The crystal structures of complexes **3**-**5** were solved by single crystal X-ray diffraction and their crystal data and structural refinement parameters are listed in the experimental section. For complex **4** two polymorphs **(4a-4b)** were obtained.

Compound **3** crystallizes in the monoclinic space group *C*2/*c* and it is isostructural with Au and Ni analogues.[29] The asymmetric unit contains half monoanionic complex with the cobalt atom at an inversion centre and one half Ph_4P^+ (Figure S1a, Table S2). In this structure, the monoanion presents the usual square planar coordination geometry, being essentially planar with the exception

of the *tert*-butyl group and the bond lengths and angles are within the expected range for other monoanionic bisdithiolate complexes. The thiophenic sulphur atom S3 presents a disorder over two possible positions (S3, S3A) of 68-32 %.

The crystal structure of complex **3** is represented in Figure 2a) and it consists of chains along the *c* axis of monoanions, $[Co(\alpha\text{-}tb\text{-}tpdt)_2]^-$. Considering the position of the thiophenic sulphur atoms with higher occupation (S3) these chains are built by a series of side-by-side short contacts ($d_{S3\cdots S3}$=3.445(2) Å, Figure 2b). With exception of these S···S contacts all other short contacts are through hydrogen atoms between cation-anion molecules, including two apical contacts C-H···Co ($d_{C\text{-}H\cdots Co}$=3.117(2) Å, Table S3). Between neighboring chains, the monoanions present, relative to each other, an angle of ~79 ° creating tunnels where the cations Ph_4P^+ are located.

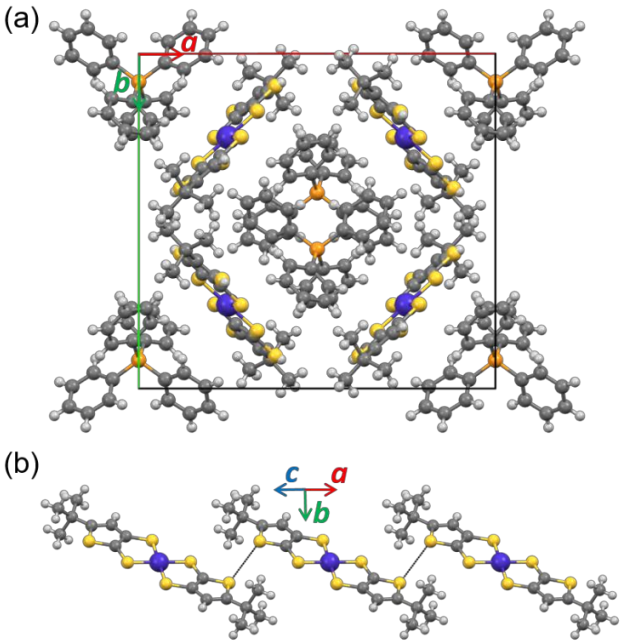

Figure 2. Crystal structure of **3**: (a) view along the *c* axis and (b) Anionic chains along *c*. The thin lines represent short S···S contacts (anions are depicted in a *trans* configuration with thiophenic sulfur atom in position S3).

Compound **5** was found to be isostructural to its Au and Ni analogues[29] and crystallizes in the triclinic system, space group $P\bar{1}$. The asymmetric unit cell contains one Ph_4P^+ at general position and two [Co(α-*dp*-tpdt)$_2$] monoanions both with the metal located in an inversion centre (Figure S1b-c, Table S4). The cobalt complexes are essentially planar, with exception of the isopropyl groups, and present a square planar coordination geometry identical to that of **3**. The bond lengths and angles are within the range observed in other monoanionic Co bisdithiolate complexes with thiophenic ligands (Table S5).[34]

The crystal structure of compound **5** is composed of anionic X-shaped chains, along *a*+*c* (Figure **3**).[29] Along the chains, two non-equivalent Co monoanions, placed side-by-side, are rotated approximately 80 ° and connected through short S···S contacts between the thiophenic sulphur atom (Table S6). All other contacts are mediated by hydrogen bonds between monoanions and cations, including with one of the cobalt atoms Co2···H21-C16 (Table S6). Between chains there is only very weak interactions mediated by the isopropyl groups. The Ph_4P^+ cations occupy the empty space in the structure between chains.

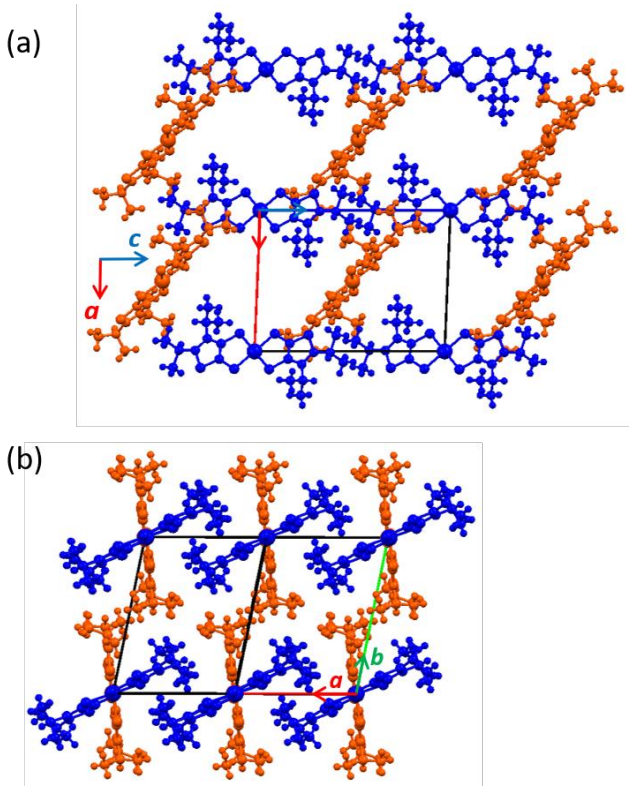

Figure 3. Crystal structure of **5** viewed (a) along *b* and (b) along *a*+*c* with Ph_4P^+ cations omitted for clarity. Non-equivalent monoanions are depicted in blue and orange.

For the iron compound **4** two polymorphs were found. Polymorph **4a** crystallizes in the monoclinic system, space group *C*2/*c*, while **4b** crystallizes in the triclinic system, space group $P\bar{1}$. In both polymorphs the asymmetric units contain one Ph_4P^+ molecule at general position and one [Fe(α-*tb*-tpdt)$_2$] dimer, with an inversion centre located between the two metal atoms (Figure S1d-e, Table S2). In **4a** and **4b** the Fe atoms present within experimental error an equal square-pyramidal (4+1) coordination geometry due to the dimerization of the Fe-bisditiolene units, with four short Fe-S bonds in the range 2.234(1)-2.262(1) Å and an apical bond at 2.479(1) Å in **4a** and 2.481(2) Å in **4b**. The iron atoms are displaced by 0.362 Å (**4a**) and 0.359 Å (**4b**) from the average plane of the four basal coordinating sulphur atoms. In spite of the bulky *tert*-butyl substituent groups in the ligands, the geometry of these complexes is comparable to that of other

dimerized Fe bisdithiolene complexes where apical Fe-S bonds have been described in the range 2.438-2.488 Å, as for instance in $(BrBzPy)_2[Fe(\alpha\text{-tpdt})_2]_2$ (2.4515(2) Å),[18] $((n\text{-}C_4H_9)_4N)Fe(mnt)_2]_2$ (2.46 Å),[36] $((ph)_4As)_2[Fe(qdt)_2]_2$ (2.4884(12) Å).[14] In both polymorphs the thiophenic sulphur atoms of the ligands present disorder over two possible positions S3-S3A and S6-S6A with occupation factors of 65-35 % and 78-22 % in **4a** and 66-34 % and 82-18 % in **4b**. In addition, **4a** also presents disorder in one of the *tert*-butyl carbon atoms (C6, C7 and C8).

The crystal structures of **4a** and **4b** are composed of alternating Ph_4P^+ cations and dimerized $[Fe(\alpha\text{-}tb\text{-tpdt})_2]_2$ complexes (Figure S2). In polymorph **4a** the dimerized Fe units are clearly isolated from each other by the cations and the bulky *tert*-butyl groups of the ligands impose a large Fe-Fe distance between dimers. Between cations and anions there are several short C-H···S contacts (Table S3). In polymorph **4b**, at variance with **4a**, the dimers $[Fe(\alpha\text{-}tb\text{-tpdt})_2]_2$ are not isolated and instead interconnected through several short S···S contacts and C-H···S hydrogen bonds (Table S3).

As previously mentioned these complexes can present unpaired electron configurations and their properties were studied by magnetic susceptibility measurements $\chi(T)$ in the range 4-300 K. Figure **4** represents the temperature dependence of the product of the paramagnetic susceptibility with the temperature ($\chi_P T$) of compounds **3** and **5** measured under a magnetic field of 0.05 T in the temperature range 2-300 K. At 299 K the values of $\chi_P T$ are 1.45 and 1.41 emu.mol/K, for **3** and **5**, corresponding to an effective moment of 3.40 and 3.36 μ_B, respectively. Upon cooling, the values of $\chi_P T$ decrease, first gradually down to 75 K and then faster below this temperature. This paramagnetic behavior clearly demonstrates that these complexes are not in a low spin (S=0) state, and a S=1 state should be considered instead. The decrease of $\chi_P T$ upon cooling can be due both to the presence of antiferromagnetic interactions (AF) or to a zero field splitting (ZFS) expected

to occur in axially distorted Co(III) complexes in a triplet state, as previously observed in monoanionic $[Co(bdt)_2]^-$ and $[Co(tdt)_2]^-$ complexes.[28]

Considering an axial local symmetry for the Co(III) center (d^6), the S=1 triplet splits into a singlet and a doublet being D the separation between them, or, the zero field splitting, ZFS.[37] Under these circumstances the product $\chi_P T$ is given by the following equation,

$$\chi_P T = \frac{2N\mu_B^2}{3k_B}\frac{g_\parallel^2 e^{-D/k_BT} + g_\perp^2(2k_BT/D)\left(1 - e^{-D/k_BT}\right)}{1 + 2e^{-D/k_BT}} \qquad (Eq.\,1)$$

where, $g_\parallel$ and $g_\perp$ are the components of the g matrix assuming an axial symmetry, N the Avogadro number, μ_B the Bohr magneton and k_B the Boltzmann constant.[28,37-38]

A fit of equation 1 to the experimental values gave the following parameters D = 27.5 K and 17.22 K, $g_\parallel$ =3.04 and 3.02 and $g_\perp$=2.64 and 2.82 for **3** and **5**, respectively. These values are comparable to those previously obtained in the few other Co(III) square planar complexes so far studied, either with dithiolene[28] or pincer type ligands,[39-40] where it was shown that this behavior and the anisotropy is strongly influenced by the nature of the ligands directly coupled to the Co atom.

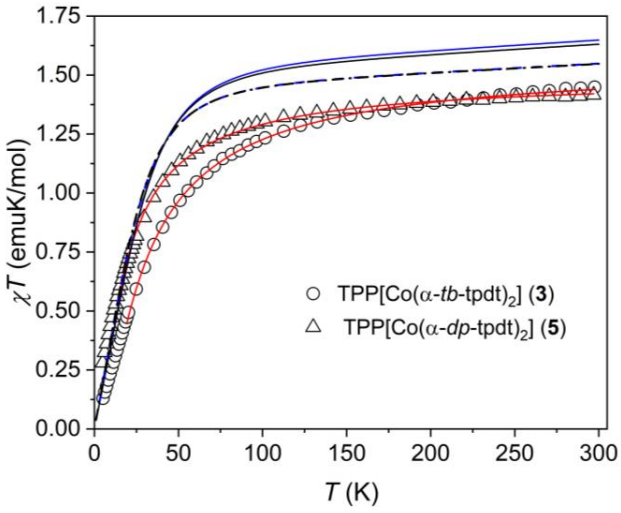

Figure 4. Temperature dependence of the $\chi_P T$ product of compounds **3** and **5** at 0.05 T. Solid red lines are fits by equation 1 and blue and black lines are calculated values using the NEVPT2 method for **3** and **5** approach with experimental structural parameters (dashed lines) and with optimized structures at DFT level (solid lines) (see text).

The faster decrease of $\chi_P T$ and the apparent larger ZFS of **3** when compared with **5** may also result from non-negligible antiferromagnetic interactions in **3**. Indeed, as previously noticed in **3** there are short S···S contacts between ligands, while in **5** the complexes are further isolated from each other.

The relative stability of the different electronic configurations and states, which can explain the observed magnetic susceptibility behavior of these cobalt complexes, were investigated by using DFT methods with the hybrid meta-GGA functional (TPSSh flavor) and multiconfigurational NEVPT2 calculations (see Computational details section). For both **3** $[Co(\alpha\text{-}tb\text{-}tpdt)_2]^-$ and **5** $[Co(\alpha\text{-}dp\text{-}tpdt)_2]^-$ complexes, at the TPSSh level, the intermediate S=1 configuration is the most stable and the S=0 configuration is the first excited singlet (and S=2 the second excited quintet) at 5.7 (15.4) and 5.6 (16.1) kcal/mol, respectively using the optimized DFT geometries (see Table S7). The equivalent spin-free energy differences at NEVPT2 level using the same optimized

geometries are 27.5 (61.7) and 28.4 (65.9) kcal/mol for **3** and **5**, respectively (see Table S8 and S9 for the reported energies including those with spin-orbit contributions). The analysis of the wave functions at CASSCF level reveals that all the states have multiconfigurational character, especially the singlet state. The largest weights of the Slater determinants are 0.30, 0.85 and 0.86 for the singlet, triplet and quintet states, respectively.

The computed dependence of the $\chi_P T$ product at spin-orbit NEVPT2 level for compounds **3** and **5** is found to be in fair agreement with the experimental data for such systems, when using calculated values under the NEVPT2 approach with experimental structural parameters (Figure 4). The computed Zero-Field Splitting parameters for both systems using the DFT optimized S=1 structure (D = +71.6 cm^{-1} (103.1 K) and D = +69.80 cm^{-1} (100.4 K) for **3** and **5** respectively) properly reproduce the sign of the D value observed but their magnitude is too large. On the other hand the calculated D values using the experimental structures (found to be around 150 kcal/mol above in energy at NEVPT2 level than those optimized with DFT) also show a comparable overestimation, but with values slightly smaller, 61.8 and 61.5 cm^{-1}, respectively for **3** and **5**. As shown in Figure 4, the calculated $\chi_P T$ values, considering isolated ions, are identical for **3** and **5**, supporting the previous assignment of the experimentally observed faster decrease upon cooling of $\chi_P T$ in **3** to the presence of antiferromagnetic interactions not taken into account in the calculations. The main contribution to the zero field splitting (Figure 5) is due to the excitations from the d_{z2}, d_{xy} orbitals to the d_{xz} orbital that correspond to a change in the $|m_l|$ value, and consequently results in a positive D value. Thus, both DFT and NEVPT2 correctly predict at qualitative level the experimental intermediate spin solution but we will focus our analysis in the NEVPT2 results due to the multiconfigurational character found.

The AILFT approach allows extracting the d-orbitals, energy and composition, using the NEVPT2 approach. In Figure 5 the orbitals are represented for the two studied molecules (**3** and **5**). As also noticed from the total energies the S=2 high spin state is very unstable due to the high energy of the d_{x2-y2} orbital. These calculations suggest that Co^{III} square planar complexes favor a triplet state (S=1) since it minimizes the interelectronic repulsion, in agreement with the few magnetically characterized compounds so far. However, if there is an electron transfer (total, partial or delocalization) from the ligand or if the Co^{III} center is reduced, then the low-spin state (S=0) becomes more stable.

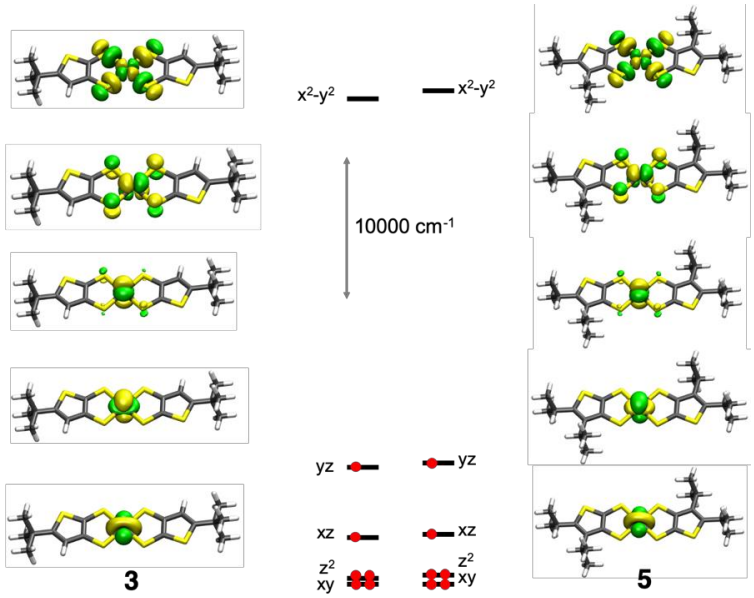

Figure 5. AILFT orbitals for **3** and **5**.

The poor stability and multiphasic nature of the Fe compounds precluded the quantitative analysis of the magnetic susceptibility of the polycrystalline material obtained. Nevertheless, magnetic susceptibility of the material resulting from the preparations of compounds **4** and **6** show clearly two contributions: one with a broad maximum at circa 150 K, typical of AF coupled dimers

as observed in most Fe bisdithiolene complexes[16,18,20,22] and a large Curie contribution, ascribed to other phases and/or impurities (Figure S3).

The Mössbauer spectra of complexes **4** and **6** were found to depend on the sample storage and preparative conditions. One single doublet could be observed in freshly prepared samples as shown in Figure 6, but other samples displayed an additional contribution ascribed to other ferric impurities due to sample decomposition (Figure S4). The Mössbauer spectra of freshly prepared samples of **4** (Figure 6) and **6** are similar, consisting of a single quadrupole doublet, both at 295 K and 4 K. The estimated parameters, isomer shift relative to α-Fe at 295 K, IS, and quadrupole splitting, QS, are summarized in Table 2. These values, at each temperature, are the same within experimental error for both compounds. The estimated IS and QS values are similar to those previously reported for dimerized S=3/2 Fe^{III} bisdithiolene complexes[20,22-23,41-42] and are higher than those observed for monomeric complexes.[14,43] The highest value of the isomer shift IS at 4 K when compared with IS at 295 K is explained by the second order Doppler shift. The decrease in QS with increasing temperature is related to thermal population of the low-lying excited electronic states in Fe^{III} S=3/2, as already explained in detail.[44] The single doublet observed for compound **4** is not surprising since the two polymorphs of this compound both present a virtually identical dimerized structure for which the same Mössbauer parameters are expected. Mössbauer results indicate that a similar dimerized structure is expected to occur in **6**, as also suggested by magnetic susceptibility results.

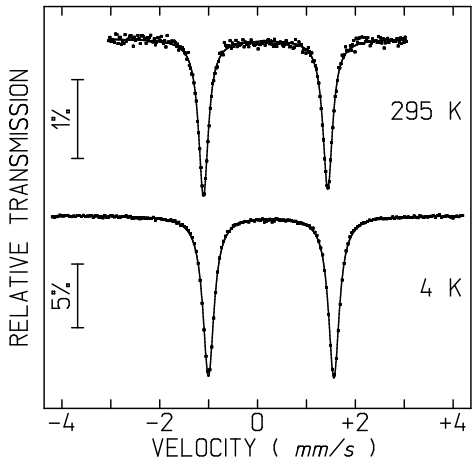

Figure 6. Mössbauer spectra of **4** taken at 295 and 4 K.

Table 2. Estimated parameters from the Mössbauer spectra taken at 295 and 4 K.

Compound	T (K)	IS (mm/s)	QS (mm/s)	Γ (mm/s)
4	295	0.28	2.54	0.24
	4	0.39	2.59	0.26
6	295	0.29	2.57	0.24
	4	0.41	2.61	0.27

IS isomer shift relative to metallic Fe at 295 K; QS quadrupole splitting; Γ peak width. Estimated standard deviations are < 0.03 mm/s.

CONCLUSIONS

In conclusion, two new monoanionic cobalt and iron complexes based on bisdithiolene-thiophenic ligands substituted with alkyl groups, *tert*-butyl and isopropyl, were prepared and characterized. The incorporation of the large alkyl groups in these dithiolene-thiophenic ligands was found to decrease their oxidation potentials, making unstable the Fe compounds, which even in solid state degrade after a few days. Compounds **3**, **4a** and **5** were found to be isostructural with

their Au and Ni analogues, and **4b** showed a complex dimerization identical to other Fe(III) bisdithiolene complexes.[18,29] The monoanionic cobalt complexes **3** and **5**, which display a square planar coordination geometry, show a paramagnetic behavior consistent with an intermediate spin (S=1) configuration in agreement with predictions of multiconfigurational NEVPT2 and DFT calculations . The positive experimental D value is also corroborated by NEVPT2 calculations, basically due to the excitations from the doubly occupied d_{z2}, d_{xy} orbitals to the singly occupied d_{xz} orbital. The crystal structure of the Fe complex **6** could not be solved, however Mössbauer spectroscopy and magnetic susceptibility data are consistent with dimerization of the Fe complexes as in **4a** and **4b**.

EXPERIMENTAL SECTION

All manipulations were carried out under strict anaerobic conditions under dry nitrogen, unless otherwise stated. All solvents were purified following the standard procedures.[45] Compounds **I** [31], **1** [30] and **2** [29] were prepared following previously reported procedures. Other chemicals were commercially obtained and used without any further purification.

Synthesis of TPP[Co(*α-tb*-tpdt)$_2$] (3). In the glovebox, proligand **1** (100 mg, 4.3×10^{-4} mol) was added to a solution of sodium methoxide (5 mL, 2 M) in methanol and stirred for 10 min. A solution of $CoCl_2\cdot6H_2O$ (51.1 mg, 1.9×10^{-4} mol) in methanol (1 mL) was then added to the previous reaction mixture. After 15 min the mixture was filtrated and a solution of tetraphenylphosphonium bromide (182 mg, 4.3×10^{-4} mol) in methanol (1 mL) was then added, without stirring. A dark blue precipitate was formed and the mixture was kept in the glovebox for an additional 12 hours. Dark blue needles shaped crystals were collected by filtration and washed

with cold MeOH (Yield: 30 %). Elemental analysis calcd (%) for $C_{40}H_{40}CoPS_6$: C 59.8, H 5.0, S 24.0; found C 59.0, H 5.0, S 23; FTIR (KBr) cm^{-1}: 3084 (arom. C-H), 1654.13 and 1420.27 (m, C=C), 1466.14 (=C-H, ring C=C), 1965.83 (-CH_3), 522.15 (S-Co), 1107.82 (P-arom.). UV-VIS λ_{max} (nm): 270, 275, 310. Crystal data and structure refinement: $C_{40}H_{40}CoPS_6$, M=802.98 $g.mol^{-1}$, monoclinic, space group *C*2/*c*, *a*=20.4344(8) Å, *b*=18.1118(7) Å, *c*=11.1487(4) Å, β=108.495(2) °, V=3914.4(3) $Å^3$, Z=4, ρ_{calc}=1.363 $g.cm^{-3}$, μ(Mo*K*α)=0.827 mm^{-1}, 11767 reflections collected, 3714 unique (R_{int}=0.0627), θ_{max}=25.679 °, R1=0.0414 using 2531 Refl. >2σ(I), ωR2=0.0987, T=150(2) K, CCDC 1996678.

Synthesis of $TPP_2[Fe(\alpha\text{-}tb\text{-}tpdt)_2]_2$ (4). This compound was prepared following the same procedure as for **3**, using $FeCl_3$ (35.2 mg, 2.1×10^{-4} mol) instead of $CoCl_2\cdot6H_2O$. The product was obtained as dark brown needles (Yield: 25 %).

Crystal data and structure refinement for complex **4a**: $C_{80}H_{80}Fe_2P_2S_{12}$, M = 1599.80 $g.mol^{-1}$, monoclinic, space group *C*2/*c*, *a*=29.8427(7) Å, *b*=15.7705(4) Å, *c*=16.7919(5) Å, β=91.6020(10) °, V=7899.8(4) $Å^3$, Z=4, ρ_{calc}=1.34 $g.cm^{-3}$, μ(Mo*K*α)=0.767 mm^{-1}, 31061 reflections collected, 7218 unique (R_{int}=0.0731), θ_{max}=25.350 °, R1=0.0651 using 5409 Refl. >2σ(I), ωR2=0.1825, T=150(2) K, CCDC 1996679.

Crystal data and structure refinement for complex **4b**: $C_{80}H_{80}Fe_2P_2S_{12}$, M = 1599.80 $g.mol^{-1}$, triclinic, space group $P\bar{1}$, *a*=12.536(2) Å, *b*=12.666(2) Å, *c*=13.025(2) Å, α=84.971(6) °, β= 68.472(5) °, γ=75.456(6) °, V=1862.3(5) $Å^3$, Z=1, ρ_{calc}=1.427 $g.cm^{-3}$, μ(Mo*K*α)=0.814 mm^{-1}, 12093 reflections collected, 6247 unique (R_{int}=0.0968), θ_{max}=25.027 °, R1=0.0658 using 3062 Refl. >2σ(I), ωR2=0.0992, T=150(2) K, CCDC 1996681.

Synthesis of $TPP[Co(\alpha\text{-}dp\text{-}tpdt)_2]$ (5). This compound was prepared following the same procedure as for **3** but uses as starting material ligand **2** instead of ligand **1**. The product was

obtained as dark blue needles (Yield: 22 %). Elemental analysis calcd (%) for $C_{44}H_{34}CoPS_6$: C 61.5, H 5.6, S 22.4; found C 59.89, H 5.76, S 22.47; FTIR (KBr) cm^{-1}: 2956.24, 2862.1 (arom.-C), 1436.26, 1419.83 (C=C), 526.25 (S-Co), 1106.92 (P-arom.). UV-VIS λ_{max} (nm): 230, 270, 318, 384, 646. Crystal data and structure refinement: $C_{44}H_{48}CoPS_6$, M = 859.08 $g.mol^{-1}$, triclinic, space group $P\bar{1}$, a=11.6764(3) Å, b=12.1136(3) Å, c=15.3974(4) Å, α=92.3830(10) °, β=91.8000(10) °, γ=102.2860(10) °, V=2124.33(9) $Å^3$, Z=2, ρ_{calc}=1.343 $g.cm^{-3}$, μ(MoKα)=0.767 mm^{-1}, 18643 reflections collected, 7987 unique (R_{int}=0.0430), θ_{max}= 25.681 °, R1=0.0408 using 6299 Refl. >2σ(I), ωR2=0.1008, T=150(2) K, CCDC 1996680.

Synthesis of TPP[Fe(α-*dp*-tpdt)$_2$] (6). This compound was prepared following the same procedure as for **4** but uses as starting material ligand precursor **2** instead of **1**. The product was obtained as black agglomerated needles (Yield: 52 %).

Cyclic Voltammetry. Cyclic voltammetry data were obtained using a BAS C3 Cell Stand. The voltammograms were obtained at room temperature with variable scan rates in the range of 20-500 $mV.s^{-1}$, platinum wire working and counter electrodes and a $Ag/AgNO_3$ (0.01 M $AgNO_3$ and 0.1 M *n*-Bu_4PF_6 in acetonitrile) reference electrode, in which the Ag^+ ion electrode was separated from the bulk solution by a Vycor™ frit. The measurements were performed on fresh solutions with a concentration of $1x10^{-3}$ M, in dichloromethane, that contained *n*-Bu_4PF_6 ($1x10^{-1}$ M) as a supporting electrolyte. Ferrocene was added directly to the solution after analysis to allow the potentials normalization *in situ*, relatively to the ferrocene/ferrocenium couple redox potential.

X-ray Diffraction. X-ray diffraction studies were performed at 150 K with a Bruker APEX-II CCD detector diffractometer using graphite monochromated MoKα radiation (λ = 0.71073 Å), in the φ and ω scans mode. A semi empirical absorption correction was carried out using SADABS[46].

Data collection, cell refinement and data reduction were done with the SMART and SAINT programs.[47] The structures were solved by direct methods using SIR97 [48] and refined by fullmatrix least-squares methods using the program SHELXL97 [49] using the winGX software package[50]. Non-hydrogen atoms were refined with anisotropic thermal parameters whereas H-atoms were placed in idealized positions and allowed to refine riding on the parent C atom. Molecular graphics were prepared using Mercury (version 4.2.0).[51]

Magnetic Measurements. The magnetic susceptibility of the different compounds was measured with a S700X SQUID magnetometer (Cryogenic Ltd) in the temperature range 4 300 K under applied magnetic fields of 0.05 T (**3** and **5**) and 0.1 T (**4** and **6**). The diamagnetic contributions from the core diamagnetism, χ_D, were estimated using the Pascal's constants for each compound as χ_D = -483 x10^{-6} emu/mol (**3** and **5**), and χ_D = -438 x10^{-6} emu/mol (**4** and **6**).

Mössbauer Spectroscopy. Mössbauer spectra were collected at 295 and 4 K in transmission mode using a conventional constant-acceleration spectrometer and a 25 mCi 57Co source in a Rh matrix. The velocity scale was calibrated using α-Fe foil. Isomer shifts, IS, are given relative to this standard at room temperature. The absorbers were obtained by gently packing the small sample crystals (5 mg of natural Fe/cm^2) into a perspex holder. Low-temperature measurements were performed with the sample immersed in liquid He in a bath cryostat. The spectra were fitted to Lorentzian lines using a non-linear least-squares method.

Computational details. DFT calculations were performed with Gaussian09 code[52] using the hybrid meta-GGA TPSSh exchange-correlational functional[53-54] combined with a triple-ζ with polarization basis set.[55] This functional provide a relatively accurate spin energetics of transition metal complexes.[56] All optimized structures are minimum verified through the corresponding vibrational analysis. The NEVPT2 calculations were performed method using the Orca computer

code.[57] In these calculations we employed the def2-TZVPP basis set,[58] including the corresponding auxiliary basis sets for correlation and Coulomb fitting. The active space contains 7 orbitals (five d orbitals of the metal and the two bonding M-L orbitals) and 10 electrons and the AILFT approach (it is mandatory to use the active space only with the five d-orbitals) was employed to extract the related orbitals.[59] Spin-Orbit coupling (SOC) correction has been included using the Quasi-Degenerate Perturbation Theory (QDPT) method as implemented in the current version of the Orca code.[59-60]

ASSOCIATED CONTENT

Supporting Information. ORTEP and atomic numbering schemes, bond lengths and short contact tables for compounds **3**-**5**. Half wave potentials of **3**-**6**. Crystal structures of polymorphs **4**. DFT computational details for **3** and **5**. Temperature dependence of the paramagnetic susceptibility $\chi_P T$ product of **4** and **6**. Mössbauer spectra of **4**. This material is available free of charge.

AUTHOR INFORMATION

Corresponding Author

* malmeida@ctn.tecnico.ulisboa.pt (M.A.), dbelo@ctn.tecnico.ulisboa.pt (D.B.)

Author Contributions

The manuscript was written through contributions of all authors. All authors have given approval to the final version of the manuscript.

Notes

The authors declare no competing financial interest.

ACKNOWLEDGMENT

This work was supported by FCT (Portugal) through contracts UID/Multi/04349/2019, PTDC/QUI-QIN/29834/2017, PTDC/QUI-QIN/32240/2017 and LISBOA-01-0145-FEDER-029666. ER and JC thank the Spanish Ministerio de Innovación, Ciencia y Universidades for the grants PGC2018-093863-B-C21, MDM-2017-0767 and Ramón y Cajal fellowship (RYC2018-024692-I), also Generalitat de Catalunya for the SGR2017-1289 grant. The authors acknowledge computer resources, technical expertise and assistance provided by the CSUC.

ABBREVIATIONS

α-tpdt, 2,3-thiophenedithiolate; bdt, 1,2-benzenedithiolato; AILFT, ab initio ligand field theory; CASSCF, complete active space self-consistent field; BrBzPy, 1-(4'-bromobenzyl)pyridinium; DFT, density functional theory; dp, diisopropyl; GGA, generalized gradient approximation; mnt, maleonitrilodithiolate, NEVPT, n-electron valence state perturbation theory; QDPT, Quasi-degenerate perturbation theory; qdt, quinoxalinedithiolate; tb, *tert*-butyl; tdt, 3,4-toluenedithiolate; tpdt, 3,4-thiophenedithiolate; TPP, tetraphenylphosphonium; TPSSh, Tao, Perdew, Staroverov, Scuseria; SOC, Spin-Orbit coupling; ZFS, zero field splitting.

REFERENCES

(1) Faulmann, C.; Cassoux, P. Solid-State Properties (Electronic, Magnetic, Optical) of Dithiolene Complex-Based Compounds. In *Dithiolene Chemistry: Synthesis, Properties, and Applications*; Stiefel, E. I., Ed; John Wiley & Sons, Inc.: USA, 2004; Vol. 52, 399-489.

(2) Robertson, N.; Cronin, L. Metal bis-1,2-dithiolene complexes in conducting or magnetic crystalline assemblies. *Coord. Chem. Rev.* **2002**, *227*, 93-127.

(3) Clemenson, P. I. The Chemistry and Solid-State properties of Nickel, Palladium and Platinum bis(maleonitrilledithiolate) compounds. *Coord. Chem. Rev.* **1990**, *106*, 171-203.

(4) Pilato, R. S.; van Houten, K. A. Metal Dithiolene Complexes in Detection: Past, Present, and Future. In *Dithiolene Chemistry: Synthesis, Properties, and Applications*; Stiefel, E. I., Ed; John Wiley & Sons, Inc.: USA, 2004; Vol. 52, 369-397.

(5) McCleverty, J. A. Metal 1,2-dithiolene and related complexes. In *Progress in Inorganic Chemistry*; Cotton, F. A., Ed.; John Wiley & Sons, Inc.: USA, 1968; Vol. 10, 49-221.

(6) Eisenberg, R. Structural Systematics of 1,1- and 1,2-Dithiolato Chelates. In *Progress in Inorganic Chemistry*; Lippard, S. J., Ed.; John Wiley & Sons, Inc.: USA, 1970; Vol. 12, 295-369.

(7) Olk, R.-M.; Olk, B.; Dietzsch, W.; Kirmse, R.; Hoyer, E. The chemistry of 1,3-dithiole-2-thione-4,5-dithiolate (dmit). *Coord. Chem. Rev.* **1992**, *117*, 99-131.

(8) White, L. K.; Belford, R. L. Quadrupole coupling constants of square-planar copper(II)-sulfur complexes from single-crystal electron paramagnetic resonance spectroscopy. *J. Am. Chem. Soc.* **1976**, *98*, 4428-4438.

(9) Schrauzer, G. N.; Mayweg, V. P. Preparation, Reactions, and Structure of Bisdithio-α-diketone Complexes of Nickel, Palladium, and Platinum. *J. Am. Chem. Soc.* **1965**, *87*, 1483-1489.

(10) Balch, A. L.; Holm, R. H. Complete Electron-Transfer Series of the [M-N_4] Type. *J. Am. Chem. Soc.* **1966**, *88*, 5201-5209.

(11) Shupack, S. I.; Billig, E.; Clark, R. J. H.; Williams, R.; Gray, H. B. The Electronic Structures of Square-Planar Metal Complexes. V. Spectral Properties of the Maleonitriledithiolate Complexes of Nickel, Palladium, and Platinum. *J. Am. Chem. Soc.* **1964**, *86*, 4594-4602.

(12) Stiefel, E. I.; Waters, J. H.; Billig, E.; Gray, H. B. The Myth of Nickel(III) and Nickel(IV) in Planar Complexes. *J. Am. Chem. Soc.* **1965**, *87*, 3016-3017.

(13) Herebian, D.; Wieghardt, K. E.; Neese, F. Analysis and Interpretation of Metal-Radical Coupling in a Series of Square Planar Nickel Complexes: Correlated Ab Initio and Density Functional Investigation of $[Ni(L^{ISQ})_2]$ (L^{ISQ}=3,5-di-*tert*-butyl-o-diiminobenzosemiquinonate(1-)). *J. Am. Chem. Soc.* **2003**, *125*, 10997-11005.

(14) Simão, D.; Ayllón, J. A.; Rabaça, S.; Figueira, M. J.; Santos, I. C.; Henriques, R. T.; Almeida, M. $[Fe(qdt)_2]^-$ salts; an undimerised Fe^{III} bisdithiolene complex stabilized by cation interactions. *CrystEngComm.* **2006**, *8*, 658-661.

(15) Yu, R.; Arumugam, K.; Manepalli, A.; Tran, Y.; Schmehl, R.; Jacobsen, H.; Donahue, J. P. Reversible, Electrochemically Controlled Binding of Phosphine to Iron and Cobalt Bis(dithiolene) Complexes. *Inorg. Chem.* **2007**, 46, 5131-5133.

(16) Balch, A. L.; Dance, I. G.; Holm, R. H. Characterization of dimeric dithiolene complexes. *J. Am. Chem. Soc.* **1968**, *28*, 1139-1145.

(17) Dance, I. G.; Miller, T. R. Reactions of dithiolene complexes with amines. I. Adducts of iron and cobalt complexes. *Inorg. Chem.* **1974**, *13*, 525-535.

(18) Neves, A. I. S.; Santos, I. C.; Belo, D.; Almeida, M. Cation and Ligand Roles in the coordination of Fe^{III} bisdithiolenes complexes; the crystal structures of $(BrBzPy)_2[Fe(qdt)_2]_2$ and $[Fe(\alpha\text{-tpdt})_2]_2^{2-}$ salts. *CrystEngComm.* **2009**, *11*, 1046-1053.

(19) Afonso, M. L.; Neves, A. I. S.; Almeida, M. Dimerisation of Fe bisdithiolene complexes; An electrochemical study. *Inorg. Chim. Acta* **2015***, 426,* 160-164.

(20) Rodrigues, J. V.; Santos, I. C.; Gama, V.; Henriques, R. T.; Waerenborgh, J. C.; Duarte, M. T.; Almeida, M. Synthesis Structure and Properties of $(HPy)_2[\{M(mnt)\}_2]_2$ compounds (M = Co or Fe, Hpy = pyridinium, mnt = maleonitrile-dithiolate). *J. Chem. Soc. Dalton Trans*. **1994**, 2655-2660.

(21) Nabarun R.; Sproules, S.; Bill, E.; Weyhermüller, T.; Wieghardt, K. Molecular and Electronic Structure of the Square Planar Bis(*o*-amidobenzenethiolato)iron(III) Anion and Its Bis(*o*-quinoxalinedithiolato)iron(III) Analogue. *Inorg. Chem.* **2008**, *47*, 10911-10920.

(22) Gama, V.; Henriques, R. T.; Bonfait, G.; Pereira, L. C.; Waerenborgh, J. C.; Santos, I. C.; Duarte, M. T.; Cabral, J. M. P.; Almeida, M. Low-dimensional molecular metals $(Per)_2M(mnt)_2$ M = Fe and Co. *Inorg. Chem.* **1992,** *31*, 2598-2604.

(23) Alves, H.; Simão, D.; Novais, H.; Santos, I. C.; Giménez-Saiz, C.; Gama, V.; Waerenborgh, J. C.; Henriques, R. T.; Almeida, M. $(n\text{-}Bu_4N)_2[Fe(dcbdt)_2]_2$. Synthesis, crystal structure and magnetic characterization. *Polyhedron* **2003**, *22*, 2481-2486.

(24) Alves, H.; Simão, D.; Santos, I. C.; Gama, V.; Henriques, R. T.; Novais, H.; Almeida, M. A Series of Transition Metal Bis(dicyanobenzenedithiolate) Complexes $[M(dcbdt)_2]$ (M = Fe, Co, Ni, Pd, Pt, Cu, Au and Zn). *Eur. J. Inorg. Chem.* **2004**, 1318-1329.

(25) Gama, V.; Henriques, R. T.; Almeida, M.; Veiros, L.; Calhorda, M. J.; Meetsma, A.; de Boer, J. L. A Novel Trinuclear Cobalt Complex: Crystal and Electronic Structure of $(Per)_4[Co(mnt)_2]_3$. *Inorg. Chem.* **1993**, *32*, 3705-3711.

(26) Gama, V.; Henriques, R. T.; Bonfait, G.; Almeida, M.; Meetsma, A.; Smaalen, S. V.; de Boer, J. L. (Perylene)Co(mnt)$_2$(CH_2Cl_2)$_{0.5}$: A Mixed Molecular and Polymeric Conductor. *J. Am. Chem. Soc.* **1992**, *114*, 1986-1989.

(27) Hatfield, W. E.; Ollis, C. R.; Jeter, D. Y. Singlet ground state in tetrabutylammonium bis(toluene-3,4-dithiolato)cobaltate. *J. Amer. Chem. Soc.* **1971**, *93*, 547-548.

(28) van der Put, P. J.; Schilperoord, A. A. Spin Delocalization in Square-Planar Spin-Triplet Benzene- and Toluenedithiolatocobaltate(III). *Inorg. Chem.* **1974**, *l13*, 2476-2481.

(29) Andrade, M. M; Silva, R. A. L.; Santos, I. C.; Lopes, E. B.; Rabaça, S.; Pereira, L. C. J.; Coutinho, J. T.; Telo, J. P.; Rovira, C.; Almeida, M.; Belo, D. Gold and nickel alkyl substituted bis-thiophenedithiolene complexes: anionic and neutral forms. *Inorg. Chem. Front.* **2017**, *4*, 270-280.

(30) Silva, R. A. L.; Vieira, B. J. C.; Andrade, M. A.; Santos, I. C.; Rabaça, S.; Belo, D.; Almeida, M. TTFs nonsymmetrically fused with alkylthiophenic moieties. *Beilstein J. Org. Chem.* **2015**, *11*, 628-637.

(31) Pérez-Benítez, A.; Tarrés, J.; Ribera, E.; Veciana, J.; Rovira, C. Improved Synthesis of the π-Electron Donor Bis(ethylenethio)tetrathiafulvalene (BET-TTF). *Synthesis* **1999**, *4*, 577-579.

(32) Belo, D.; Alves, H.; Lopes, E. B.; Duarte, M. T.; Gama, V.; Henriques, R. T.; Almeida, M.; Pérez-Benítez, A.; Rovira, C.; Veciana, J. Gold Complexes with Dithiothiophene Ligands: A Metal Based on a Neutral Molecule. *Chem. Eur. J.* **2001**, *7*, 511-519.

(33) Afonso, M. L.; Neves, A. I. S.; Almeida, M. Dimerisation of Fe bisdithiolene complexes: An electrochemical study. *Inorg. Chim. Acta* **2015**, *426*, 160-164.

(34) Belo, D.; Figueira, M. J.; Mendonça, J.; Santos, I. C.; Almeida, M.; Henriques, R. T.; Duarte, M. T.; Rovira, C.; Veciana, J. Copper, Cobalt and Platinum Complexes with Dithiothiophene Based Ligands. *Eur. J. Inorg. Chem.* **2005**, 3337-3345.

(35) Gagne, R. R.; Koval, C. A.; Lisensky, G. C. Ferrocene as an internal standard for electrochemical measurements. *Inorg Chem.* **1980**, *19*, 2854-2855.

(36) Hamilton, W. C.; Bernal, I. Crystal and molecular structure of the tetra-n-butyl ammonium salt of bis(maleonitriledithiolato)iron(III)-a pyramidal iron(III) dimer. *Inorg. Chem.* **1967**, *6*, 2003-2008.

(37) Carlin, R. L. Paramagnetic susceptibilities. *J. Chem. Educ.* **1966**, *43*, 521-525.

(38) Carlin, R. L. *Magnetochemistry*. Springer-Verlag Berlin Heidelberg, 1986.

(39) García-Monforte, M. A.; Ara, I.; Martín, A.; Menjón, B.; Tomás, M.;Alonso, P. J.; Arauzo, A. B.; Martínez, J. I.; Rillo, C. Homoleptic Organocobalt(III) Compounds with Intermediate Spin. *Inorg. Chem*. **2014**, *53*, 12384-12395.

(40) Lagaditis, P. O.; Schluschaß, B.; Demeshko, S.; Würtele, C.; Schneider, S. Square-Planar Cobalt(III) Pincer Complex. *Inorg. Chem*. **2016**, *55*, 4529-4536.

(41) De Boer, E.; De Vries, J. L. K. F.; Trooster, J. M. A Mössbauer Study of Solvation Effects of Five-Coordinated Iron(III) Complexes with Sulfur-Containing Ligands. *Inorg. Chem.* **1971**, *10*, 81-85.

(42) Cerdeira, A. C.; Simão, D.; Santos, I. C.; Machado, A.; Pereira, L. C. J.; Waerenborgh, J. C.; Henriques, R. T.; Almeida, M. (n-Bu_4N)[$Fe(cbdt)_2$]; Synthesis, crystal structure and magnetic characterisation of a new Fe^{III} bisdithiolene complex. *Inorg. Chim. Acta* **2008**, *361*, 3836-3841.

(43) Dalziel, J. A. W.; Donaldson, J. D.; Mehta, B. D.; Tricker, M. J. ^{57}Fe Mössbauer spectra of some quinoxaline-2,3-dithiolate complexes of iron. *J. Inorg. Nucl. Chem.* **1973**, *35*, 3811-3814.

(44) Bancroft, G.M. Mössbauer Spectroscopy: An Introduction for Inorganic Chemists and Geochemists. McGraw Hill, London, 1973.

(45) Perrin, D. D.; Armarego, W. L. F. Purification of Laboratory Chemicals, 3rd ed.; Pergamon Press: Oxford, UK, 1988.

(46) Sheldrick, G. M. SADABS, Bruker AXS Inc., Madison, Wisconsin, USA, 2004.

(47) Bruker. SMART and SAINT. Bruker AXS Inc., Madison, Wisconsin, USA, 2008.

(48) Altomare, A.; Burla, M. C.; Camalli, M.; Cascarano, G.; Giacovazzo, G.; Guagliardi, A.; Moliterni, A. G. G.; Polidori, G.; Spagna, R. *SIR*97: a new tool for crystal structure determination and refinement. *J. Appl. Cryst.*, **1999**, *32*, 115-119.

(49) Sheldrick, G. M. A short history of *SHELX*. *Acta Cryst.* **2008**, *A64*, 112-122.

(50) Farrugia, L. J. *WinGX* and *ORTEP* for *Windows:* an update. *J. Appl. Cryst.* **2012**, *45*, 849-854.

(51) Macrae, C. F.; Bruno, I. J.; Chisholm, J. A.; Edgington, P. R.; McCabe, P.; Pidcock, E.; Rodriguez-Monge, L.; Taylor, R.; van de Streek, J.; Wood, P.A. Mercury CSD 2.0 - new features for the visualization and investigation of crystal structures. *J. Appl. Cryst.* **2008**, *41*, 466-470.

(52) Frisch, M. J.; Trucks, G. W.; Schlegel, H. B.; Scuseria, G. E.; Robb, M. A.; Cheeseman, J. R.; Scalmani, G.; Barone, V.; Mennucci, B.; Petersson, G. A.; Nakatsuji, H.; Caricato, M.; Li, X.;

Hratchian, H. P.; Izmaylov, A. F.; Bloino, J.; Zheng, G.; Sonnenberg, J. L.; Hada, M.; Ehara, M.; Toyota, K.; Fukuda, R.; Hasegawa, J.; Ishida, M.; Nakajima, T.; Honda, Y.; Kitao, O.; Nakai, H.; Vreven, T.; Montgomery J. A, Jr.; Peralta, J. E.; Ogliaro, F.; Bearpark, M.; Heyd, J. J.; Brothers, E.; Kudin, K. N.; Staroverov, V. N.; Kobayashi, R.; Normand, J.; Raghavachari, K.; Rendell, A.; Burant, J. C.; Iyengar, S. S.; Tomasi, J.; Cossi, M.; Rega, N.; Millam, N. J.; Klene, M.; Knox, J. E.; Cross, J. B.; Bakken, V.; Adamo, C.; Jaramillo, J.; Gomperts, R.; Stratmann, R. E.; Yazyev, O.; Austin, A. J.; Cammi, R.; Pomelli, C.; Ochterski, J. W.; Martin, R. L.; Morokuma, K.; Zakrzewski, V. G.; Voth, G. A.; Salvador, P.; Dannenberg, J. J.; Dapprich, S.; Daniels, A. D.; Farkas, Ö.; Foresman, J. B.; Ortiz, J. V.; Cioslowski, J.; Fox, D. J. *Gaussian 09 (Revision A.1)*, Wallingford, CT, 2009.

(53) Staroverov, V. N.; Scuseria, G. E.; Tao, J. M.; Perdew, J. P., Comparative assessment of a new nonempirical density functional: Molecules and hydrogen-bonded complexes. *J. Chem. Phys.* **2003**, *119*, 12129-12137.

(54) Tao, J. M.; Perdew, J. P.; Staroverov, V. N.; Scuseria, G. E., Climbing the density functional ladder: Nonempirical meta-generalized gradient approximation designed for molecules and solids. *Phys. Rev. Lett.* **2003**, *91*, 146401.

(55) Schafer, A.; Huber, C.; Ahlrichs, R., Fully-optimized contracted gaussian-basis sets of triple zeta valence quality for atoms Li to Kr. *J. Chem. Phys.* **1994**, *100*, 5829-5835.

(56) Cirera, J.; Via-Nadal, M.; Ruiz, E., Benchmarking Density Functional Methods for Calculation of State Energies of First Row Spin-Crossover Molecules. *Inorg. Chem.* **2018**, *57*, 14097-14105.

(57) Neese, F., Software update: the ORCA program system, version 4.0. *WIREs Computational Molecular Science* **2018**, *8*, e1327.

(58) Weigend, F.; Ahlrichs, R., Balanced basis sets of split valence, triple zeta valence and quadruple zeta valence quality for H to Rn: Design and assessment of accuracy. *Phys. Chem. Chem. Phys.* **2005**, *7*, 3297-3305.

(59) Atanasov, M.; Aravena, D.; Suturina, E.; Bill, E.; Maganas, D.; Neese, F., First principles approach to the electronic structure, magnetic anisotropy and spin relaxation in mononuclear 3d-transition metal single molecule magnets. *Coord. Chem. Rev.* **2015**, *289*, 177-214.

(60) Hose, G.; Kaldor, U. Quasidegenerate Perturbation Theory. *J. Phys. Chem.* **1982**, *86*, 2133-2140.

SYNOPSIS

TPP[Co(α-*tb*-tpdt)$_2$] and TPP[Co(α-*dp*-tpdt)$_2$] are monoanionic cobalt complexes in a square planar coordination geometry. The studies herein reported revealed an intermediate spin electronic configuration (S=1). The results are supported by multiconfigurational DFT calculations and experimental data. The magnetic susceptibility showed a behavior dominated by antiferromagnetic interactions, with room temperature magnetic moments of 3.40 μB and 3.36 μB, respectively.